RESEARCH ARTICLE | FEBRUARY 05 2019

Local mean age of melt: New approaches for die optimisation

J. Kummerow; J. Wortberg

AIP Conf. Proc. 2065, 030011 (2019)
https://doi.org/10.1063/1.5088269

Local Mean Age of Melt: New Approaches for Die Optimisation

J. Kummerow[a] and J. Wortberg

University of Duisburg-Essen, Institute of Product Engineering, Engineering Design and Plastics Machinery (IPE-KKM), Duisburg, Germany

[a]*jan.kummerow@uni-due.de*

Abstract. In the design process of extrusion dies, the utilisation of computational fluid dynamics (CFD) is state of the art. To evaluate the distribution quality of different die geometries, the circumferential velocity at die exit is the most commonly used criterion. In conjunction with maximal and minimal wall shear stresses, it is possible to define an overall quality score for each die based on CFD results.

In the face of shrinking batch sizes and the demand for more frequent changes of colour or material, the localisation of stagnation zones becomes more and more important. These stagnation zones lead to higher residence times of the polymer melt inside the die. Thus, it takes longer to clean the die and it subsequently requires more purging material. Therefore, new quality criteria for extrusion dies should be taken into consideration to detect regions with high residence times. In post processing, streamlines could be used to track down stagnation zones qualitatively. However, this method involves user interaction as well as additional computations. To obtain the spatial distribution of residence times from streamlines, further calculations are required, making this method even less suitable for automatic geometry optimisations. Instead, it is proposed to use the concept of the local mean age of melt, which is directly obtained from the numerical solver calculating an additional transport equation. The local age of the melt is available as a scalar field, making it possible to estimate e.g. global extreme values. Based on the mean age, new quality criteria are developed for the automatic optimisation of spiral mandrel dies. This approach ensures that problematic spots such as the feed-in region of the spiral grooves can be safely detected and locally optimised.

Keywords: mean age theory, residence time distribution, spiral mandrel die optimization, extrusion die.
PACS: 81.20.Hy, 83.50.Uv, 07.05.Tp, 87.55.de

INTRODUCTION

In the face of shrinking batch sizes and the demand for more frequent changes of colour or material, the localisation of stagnation zones becomes more and more important. These stagnation zones lead to higher residence times of the polymer melt inside the die. Thus, it takes longer to clean the die and it subsequently requires more purging material. In post processing, streamlines could be used to track down stagnation zones qualitatively. However, this method involves user interaction as well as additional computations. As an alternative, this paper proposes to use the mean age of melt, explained briefly in the first section. This concept was already developed in the 1950s by Danckwerts [1] and Spalding [2].

THE THEORY OF MEAN AGE

The residence time distribution (RTD) can be obtained by conducting the following experiment [3]: Let us assume, we have a stationary fluid flow through a pipe. At time $t_0 = 0$, we change abruptly from material A to material B, having the same flow characteristics and differ in colour only. Then, we measure continuously the concentration of material B at the outlet of the pipe. Examples of the resulting curves are depicted in Figure 1. For plug flow types, a curve similar to Figure 1 (a) may be obtained, shaped like the step input. However, for a more realistic flow profile, which will slow down at wall (no-slip condition), the change of concentration will take a measureable amount of time, resulting in a smooth transition (Figure 1 (b)). Both functions are centered around the same mean time of about 60 s. Mathematically this cumulative distribution function (CDF) can be written as

Proceedings of PPS-34
AIP Conf. Proc. 2065, 030011-1–030011-5; https://doi.org/10.1063/1.5088269
Published by AIP Publishing. 978-0-7354-1793-9/$30.00

$$F(t) = \frac{\int_0^t C_{out}\, dt'}{\int_0^\infty C_{out}\, dt} \quad (1)$$

with the exit concentration C_{out} and time t. Its derivative f is the probability density function (PDF)

$$f(t) = \frac{dF}{dt} = \frac{C_{out}}{\int_0^\infty C_{out}\, dt}, \quad (2)$$

also depicted in Figure 1. The mean residence time is then the first momentum of the f-function

$$\tau = \frac{\int_0^\infty t\, C_{out}\, dt}{\int_0^\infty C_{out}\, dt} = \int_0^\infty t \cdot f\, dt. \quad (3)$$

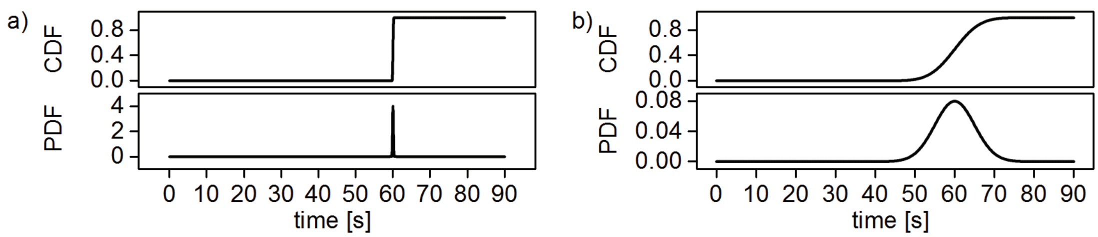

FIGURE 1. Example for a Cumulative Distribution Function (CFD) and a Probability Density Function (PDF) for (a) plug flow case and (b) real flow case.

It is important to mention that these representations of the RTD are solely defined at the exit indicated by the term C_{out}. The RTD's shape may give hints to the occurrence of stagnation zones, e.g. by its width or the occurrence of a significant tail, but this is mostly speculation and the location of these regions cannot be determined from it [3]. This motivates the need for an spatial distribution of the residence time, which shall be called from now on 'age' to distinguish it from the above defined exit distribution.

The mathematical definition of the mean age distribution $\theta(\boldsymbol{x})$ derives from Eq. (3) as function of its spatial position x

$$\theta(\boldsymbol{x}) = \frac{\int_0^\infty t\, C(\boldsymbol{x},t)\, dt}{\int_0^\infty C(\boldsymbol{x},t)\, dt}. \quad (4)$$

Spalding [2] proposes the following equation to describe the transport of tracers by convection and diffusion

$$\frac{\partial C}{\partial t} = \nabla \cdot (\Gamma \nabla C) - \nabla \cdot (\boldsymbol{u} C) \quad (5)$$

with $\boldsymbol{u}$, local convective velocity vector, Γ the local diffusivity and ∇ the nabla operator. The mean age is then obtained by multiplying Eq. (5) by the time t and integration from $t = 0$ to $t = \infty$:

$$-\int_0^\infty C\, dt = \nabla\left(\Gamma\, \nabla \int_0^\infty C\, t\, dt\right) - \nabla\left(\boldsymbol{u} \int_0^\infty C\, t\, dt\right). \quad (6)$$

Following Sandberg [4], we then divide the whole equation by its left hand side and substitute Eq. (4) to obtain the transport equation for the mean age:

$$\nabla(\boldsymbol{u}\theta - \Gamma \nabla \theta) = 1. \quad (7)$$

Equation (7) has the same conservative form as the transport equations for mass, momentum and energy solved by numerical finite volume method (FVM) solvers like Fluent. The necessary boundary conditions are

$$\theta = 0, \text{ at inlet}$$
$$\boldsymbol{n} \cdot \nabla a = \frac{\partial a}{\partial x_n} = 0, \text{ on solid walls} \quad (8)$$

This method is orders of magnitude cheaper in terms of needed computational efforts and therefore faster than conventional transient methods. As shown by others [3,5,6], the accuracy of the mean age method is nevertheless comparable to time-dependent methods.

APPLICATION TO SPIRAL MANDREL DIES

The commercial CFD solver Fluent is easily extendable by user-defined functions written in C, used in this work to integrate Eq. (7). It calculates the mean age as scalar field right after the velocity vector field. The post processor can handle it like other common quantities such as temperature or pressure. For instance, the spatial distribution of the mean age can be visualised by contour plots, isovolumes and alike.

This study uses a spiral mandrel die with the following design specifications: The overall height of the die is 380 mm, the exit diameter of the mandrel is 100 mm, and the spiral distribution system consists of four spiral grooves, which have a wrap angel of approx. 270 degree and a height of approx. 120 mm. From the star-shaped pre-distributor system, featuring a 90-degree elbow pipe, the channels ascend at a 45-degree angle to the spiral distributor. Figure 2 depicts the geometry used.

FIGURE 2. Geometry of the spiral mandrel die used in this study.

Due to the 90-degree elbow pipe, it is not possible to facilitate the geometry by using the periodicity of the spiral mandrel die and the numerical simulation needs the whole die meshed. The meshing was done with a mean size of approx. 1 mm, with hexa-cells where possible and tetras otherwise, and applied inflation layers to improve numerical accuracy. Overall, 3.5 Mio. cells were created for the entire fluid volume. The fluid flow simulations were conducted under the inlet-flow boundary condition of $15\,kg/h = 4.167 \cdot 10^{-3}\,kg/s$, constant temperature and zero pressure at the outlet. A material with virtual properties representative for polyolefin grades was used.

As mentioned before, the use of contour plots is one possibility to visualise the spatial distribution of the mean age of melt. They reveal the higher residence times of the flow near the outer and inner brim due to the wall-stick of the flow, whereas the main flow appears to be not noticeably affected. However, further conclusions can hardly be made, as the circumferential distribution seems to be qualitatively constant. Figure 3 (a) shows the mean age evaluated over the circumference of three circular polylines positioned evenly at the inner and outer brim, as well as in the middle of the annular gap. As expected, the middle flow has the lowest residence times of about 100 s, whereas the boundary flows have higher residence times of approx. 135 s. The evaluation explicitly at these circular lines reveals that the circumferential distribution is not as even as one could think by just looking at the contour plot of Figure 3 (a). The curve features four minima and maxima regions, which correspond to the four spiral mandrels of the die. The flow length of the spiral flow is much longer than for the gap flow, resulting in deviations in residence time. Further, the age maxima of the outer and inner curves are shifted by approx. 30 degrees, indicating their origin from gap and spiral flow as well.

Apart from the more or less periodic repeating maxima and minima, there is also a general tendency for higher residence times between 0 and 180 degrees and lower between 180 and 360 degrees. By standardising the mean age to the mean value, it is possible to plot all curves together (see Figure 3 b), showing this tendency more clearly.

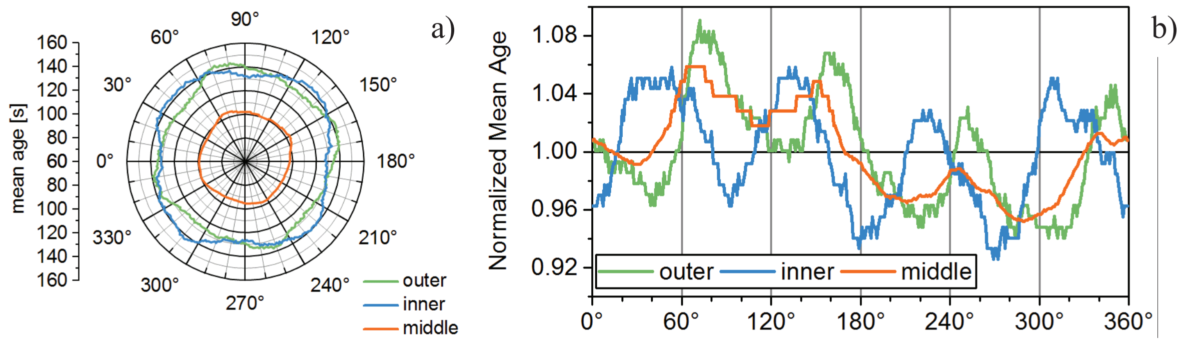

FIGURE 3. (a) Mean age over the circumference of three circular polylines, positioned evenly at the inner and outer brim, as well as in the middle of the annular gap. (b) Normalized mean age over circumference at the outer and inner brim as well as in the middle of the gap

The by far greatest proportion of melt is exiting the die through the middle flow, thus its residence time is dominating the mean exit age, which is equal to the mean residence time, $\bar{\theta}_{exit} = \tau = 105.63\ s$. Between 60 and 180 degree, the mean age of the middle flow becomes maximal. Streamlines starting in this region of the outlet plane in backward direction then expose the cause for higher ages of melt at the exit. Figure 4 shows an isometric view as well as a cross-sectional view through infeed axis. Clearly, the exiting flow with higher residence times correlates to areas with low velocity at the redirection section of the infeed. These regions also show low wall shear stresses known for bad purging behaviour. The streamlines leave the spiral channel relatively quick and run through the gap for the remaining die. In this case, the longer flow path through the channels are not responsible for the effect of higher exit mean age. With the knowledge obtained by this analysis, a precise improvement of the infeed's melt transport is possible to reduce the residence time of melt running through its boundary regions with low velocity.

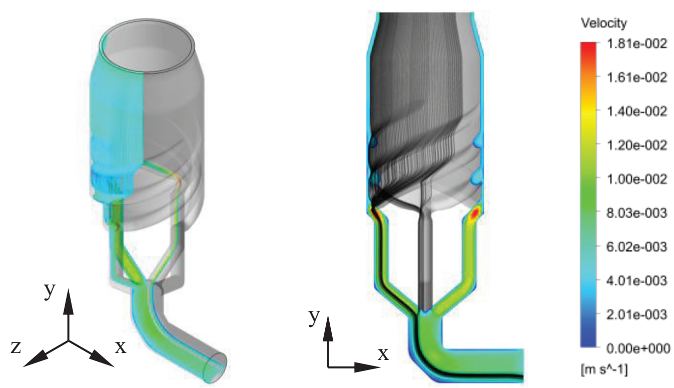

FIGURE 4. Streamlines starting at the outlet in areas with high residence times according to Fig. 3. Left: Isometric view with streamlines coloured according to local velocity. Right: Cross-section view along the infeed axis with velocity plotted.

However, this type of analysis is not applicable to automatic optimisations e.g. of the channel depth or gap width. In these cases, a single scalar value is necessary for evaluation and comparison of die designs. This characteristic value, which we will call quality criterion, scales ideally from zero (best) to one (worst) and yet has to describe the whole residence time distribution. Then, an optimiser can use it in order to minimise the associating zones of melt stagnation.

The simplest quality criteria imaginable is the ratio of maximal and minimal age, as they are directly available in post processing. However, due to the wall-stick condition implausibly high mean ages are observable in proximity to walls. Some way to omit these data would be necessary, for example achieved by evaluating the maximum age at a user-defined surface shifted from the wall far enough.

Instead, this work makes use of average values to ensure that numerically erroneous data does not distort the results. For that purpose, the outlet surface is divided in stripes e.g. of ten degrees at which the massflow-averaged age is calculated. Similar to the evaluation of circumferential distribution of the exit melt flow, it is possible to propose a quality criterion of the form

$$Qa_E = \frac{\max(\bar{\theta}_i)-\min(\bar{\theta}_i)}{\bar{\theta}} \quad (9)$$

where $\bar{\theta}_i$ is the average mean age at the particular plane and $\bar{\theta}$ is the average over the whole exit plane.

Although it is possible to improve purging times with Qa_E, the criterion only uses exit ages and therefore cannot localise stagnation zones directly. To do so, a spatially defined quality criterion is necessary which is also compressible to a single value. For this purpose, a concept developed by Spalding [2] is adapted for polymer flows we like to call fluid change effectiveness (FCE):

$$\varepsilon = \frac{\tau}{\theta} = \frac{\bar{\theta}_{exit}}{\theta}. \quad (10)$$

Note, that the FCE is using the local mean age as denominator and has to be evaluated separately in every cell of the fluid domain. Then, ε describes how often a local volume is purged in the time a plug flow would need to pass through the whole die. If ε is greater than one, the volume is purged at least once, while values smaller than one indicate partial purging. Therefore, it is feasible to obtain the volume occupied by cells partially purged. This dead volume V_ε normalised to the total volume V_{total} forms another quality criterion:

$$Q\varepsilon = \frac{V_\varepsilon}{V_{total}}. \quad (11)$$

CONCLUSION

Exemplary for one spiral mandrel die, this paper presents a CFD-study featuring the usage of the mean age of melt to investigate the spatial residence time distribution and to identify stagnation zones. In the course of this investigation utilising a combination of contourplots and streamlines, the infeed region was located as problematic in terms of purging behaviour. Then, some quality criteria for evaluation and comparison of die designs were presented. The evaluation of these criteria for the geometry shown in Figure 2 in comparison with the same die design without the redirection of the infeed shows Table 1. As expected, the criteria decrease due to the absence of stagnation regions, which are located in the infeed.

TABLE 1. Comparison of quality criteria.

	With redirection	Without redirection
Qa_E	10.05 %	5.78 %
$Q\varepsilon$	8.68 %	8.20 %

Numerical optimisers can use these criteria to improve the purging behaviour of extrusion dies by changing certain geometric details such as the depth of the spiral grooves. In the face of market demands for more flexibility of extrusion dies, the design process should seriously consider the mean age distribution.

ACKNOWLEDGEMENTS

We like to thank the German National Science Foundation (Deutsche Forschungsgemeinschaft, DFG) for funding this research project titled “Automated generation of virtual prototypes for extrusion dies”, Project-No.: WO 302/48-2 and KO 1620/12-2.

REFERENCES

1. P. V. Danckwerts, Chemical Engineering Science **2**, 1–13 (1953).
2. D. B. Spalding, Chemical Engineering Science **9**, 74–77 (1958).
3. M. Liu and J. N. Tilton, AIChE J. **56**, 2561–2572 (2010).
4. M. Sandberg, Building and Environment **16**, 123–135 (1981).
5. D. C. Russ and R. E. Berson, Chemical Engineering Science **141**, 1–7 (2016).
6. J.-N. Baléo and P. Le Cloirec, AIChE J. **46**, 675–683 (2000).